Inorg. Chem. **2005**, *44*, 7751–7761

Synthesis, Crystal Structure, and Solution Stability of Keggin-Type Heteropolytungstates $(NH_4)_6Ni^{II}_{0.5}[\alpha\text{-}Fe^{III}O_4W_{11}O_{30}Ni^{II}O_5(OH_2)]\cdot nH_2O$, $(NH_4)_7Zn_{0.5}[\alpha\text{-}ZnO_4W_{11}O_{30}ZnO_5(OH_2)]\cdot nH_2O$, and $(NH_4)_7Ni^{II}_{0.5}[\alpha\text{-}ZnO_4W_{11}O_{30}Ni^{II}O_5(OH_2)]\cdot nH_2O$ ($n \approx 18$)†

Heiko Weiner,‡ Hans-Joachim Lunk,*,§ Rita Friese,£ and Hans Hartl£

The Dow Chemical Company, Building 1776, Midland, Michigan 48674, Osram Sylvania, Inc., Hawes Street, Towanda, Pennsylvania 18848, and Institut für Chemie der Freien Universität, Fabeckstrasse 34-36, D-14195 Berlin, Germany

Received December 30, 2004

Reaction of acidified (pH ≈ 7) sodium tungstate solutions with transition metal cations (Fe^{3+}, Ni^{2+}, Zn^{2+}, Co^{2+}) leads to the formation of transition-metal-disubstituted Keggin-type heteropolytungstates with 3d-metal ions distributed over three different positions. A detailed investigation of the synthesis conditions confirmed that the complexes could equally be obtained using aqueous solutions of either $Na_2WO_4\cdot 2H_2O$ (sodium monotungstate) at pH ≈ 7, $Na_6[W_7O_{24}]\cdot\sim 14H_2O$ (sodium paratungstate A), or $Na_{10}[H_2W_{12}O_{42}]\cdot 27H_2O$ (sodium paratungstate B) as starting materials. Three complexes, $(NH_4)_6Ni^{II}_{0.5}[\alpha\text{-}Fe^{III}O_4W_{11}O_{30}Ni^{II}O_5(OH_2)]\cdot 18H_2O$, $(NH_4)_7Zn_{0.5}[\alpha\text{-}ZnO_4W_{11}O_{30}\ ZnO_5(OH_2)]\cdot 18H_2O$, and $(NH_4)_7Ni^{II}_{0.5}[\alpha\text{-}ZnO_4W_{11}O_{30}Ni^{II}O_5(OH_2)]\cdot 18H_2O$ were isolated in crystalline form. X-ray single-crystal structure analysis revealed that the solid-state structures of the three compounds consist of four main structural fragments, namely $[MO_4W_{11}O_{30}M'O_5(OH_2)]^{n-}$ (Keggin-type, α-isomer) heteropolytungstates, hexaquo metal cations, $[M''(OH_2)_6]^{2+}$, ammonium–water cluster ions, $[(NH_4^+)_8(OH_2)_{12}]$, and additional ammonium cations and water molecules. The 3d metals occupy the central (tetrahedral, M) and the peripheral (octahedral, M′) positions of the Keggin anion, as well as cationic sites (M″) outside of the polyoxotungstate framework. UV–vis spectroscopy, solution (^1H, ^{183}W) and solid-state (^1H) NMR, and also chemical analysis data provided evidence that the 3d-metal-disubstituted Keggin anions do not exist in solution but are being formed only during the crystallization process. Investigations in the solid state and in solution were completed by ESR, IR, and Raman measurements.

Introduction

Polyoxometalates (POMs)[1] are polyatomic, condensed oligomeric aggregates of transition metals and oxide ions held together by metal−oxygen bonds. Polyoxoanions are also known as soluble metal oxide analogues, which resemble discrete fragments of the solid metal-oxide component of insoluble catalysts. Because of this resemblance, POMs are of considerable interest as catalysts and catalyst−support materials.[2]

There is little doubt that the Keggin[3]-type polyoxotungstates (POTs) are the most extensively studied polyanions in POM chemistry. A nonmetal (most commonly Si or P) or metal (e.g., Al, Fe, Co) is located in the central tetrahedral cavity of the Keggin structure $[EO_4W_{12}O_{36}]^{n-}$. Two of the

† In memoriam Professor Joachim Fuchs.

* To whom correspondence should be addressed. Phone: (570) 268-5503. Fax: (570) 268-5350. E-mail: hans-joachim.lunk@sylvania.com.

‡ The Dow Chemical Company.

§ Osram Sylvania.

£ Institut für Chemie der Freien Universität.

(1) Lead references to polyoxometalates and their broad range of chemistries: (a) Pope, M. T. *Heteropoly and Isopoly Oxometalates*; Springer-Verlag: New York, 1983. (b) Pope, M. T.; Müller, A. *Angew. Chem., Int. Ed. Engl.* **1991**, *30*, 34−48. (c) *Polyoxometalates: From Platonic Solids to Anti-Retroviral Activity*; Proceedings of the July 15−17, 1992 Meeting at the Center for Interdisciplinary Research in Bielefeld, Germany; Müller, A., Pope, M. T., Eds.; Kluwer Publishers: Dordrecht, The Netherlands, 1992. (d) Hill, C. L.; Ed. Polyoxometalates. *Chem. Rev.* **1998**, *98*, 1−387.

(2) For recent reviews of heteropolyoxoanions in homogeneous and heterogeneous catalysis, see: (a) Hill, C. L.; Prosser-McCartha C. M. *Coord. Chem. Rev.* **1995**, *143*, 407−455. (b) A series of 34 recent papers devoted to polyoxoanions in catalysis is given in: Hill, C. L. *J. Mol. Catal.* **1996**, *114*, 1−365, (c) Okuhara, T.; Mizuno, N.; Misono, M. *Adv. Catal.* **1996**, *41*, 113−252. (d) Kozhevnikov, I. V. *Catal. Rev. Sci. Eng.* **1995**, *37*, 311−352. (e) Neuman, R. *Prog. Inorg. Chem.* **1998**, *47*, 317−370.

(3) (a) Keggin, J. F. *Nature* **1933**, *131*, 908−909. (b) Keggin, J. F. *Proc. R. Soc. A* **1934**, *144*, 75−100.

10.1021/ic048155l CCC: $30.25
Published on Web 10/06/2005

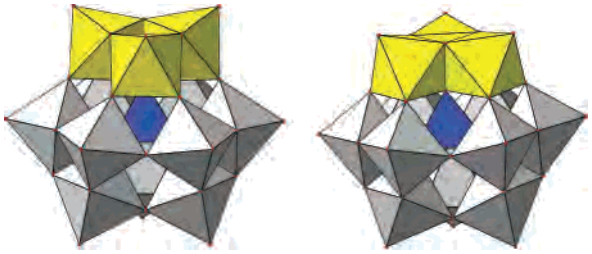

Figure 1. Polyhedral representation of the α- and *β*-isomers of the Keggin structure $[EO_4W_{12}O_{36}]^{n-}$. The *β*-isomer (right) is obtained by rotating one W_3O_{13} group of the α-isomer (left) by 60°.

five Baker−Figgis isomers[4] of the Keggin structure are shown in Figure 1.

The synthesis of transition-metal-substituted Keggin anions has been of special interest during recent years, since these compounds show potential as robust and oxidation-resistant ligands and catalysts in the oxidation of alkanes and olefins with either hydrogen peroxide or molecular oxygen.[2,5] The preparation of monosubstituted Keggin anions is usually based on so-called *lacunary* anions such as $[\alpha\text{-}PO_4W_{10}O_{35}]^{7-}$ and $[\alpha\text{-}SiO_4W_{11}O_{35}H]^{7-}$.[5] The lacunary anions have well-defined metal-cation binding sites[6] and are useful synthons for the preparation of new or substituted POTs. For example, the addition of divalent transition metal ions (i.e., Ni^{2+}) to a lacunary POT such as undecatungstosilicate results in the formation of $[\alpha\text{-}SiO_4W_{11}O_{30}Ni^{II}O_5(OH_2)]^{6-}$, which can easily be isolated as the potassium salt.[7] The synthesis of multiple transition-metal-substituted Keggin anions based on the completion of nona- and decatungstosilicates or -phosphates has also been reported.[8]

Besides this well-known class of polyoxoanions,[9] several other Keggin-type POTs have been described which contain two transition metals but neither silicon nor phosphorus in the central cavity. In these anions, one of the transition metal ions occupies the central tetrahedron of the Keggin structure and the second ion is located in an octahedral position replacing W in a $\{WO_6\}$ octahedron. One of the best-known POTs in this class is probably $[Co^{II}O_4W_{11}O_{30}Co^{II}O_5(OH_2)]^{8-}$.[10,11] Other POTs containing combinations of Fe^{3+}, Ni^{2+}, Zn^{2+}, Co^{2+}, and Co^{3+} as heteroelements were assumed to have similar compositions.[7] The synthesis of these anions is distinctly different since lacunary Keggin-type anions with transition metals as heteroelements are either unknown or of low stability.[12] Addition of transition metal salts to aqueous, weakly basic (pH 8−9) monotungstate solutions result in the precipitation of the corresponding metal oxide hydrates; hence, an acidification to a pH of 6.5−7.5 is first carried out before the transition metal salts can be added. Initial acidification of WO_4^{2-} yields a mixture of coexisting isopolytungstates, i.e., $[H_2W_6O_{22}]^{6-}$, $[W_7O_{24}]^{6-}$ (paratungstate A), $[HW_7O_{24}]^{5-}$, and $[H_2W_{12}O_{42}]^{10-}$ (paratungstate B).[13] The classic POT $[Co^{II}O_4W_{11}O_{30}Co^{II}O_5(OH_2)]^{8-}$, for example, is then obtained by addition of cobalt(II) acetate at a pH of ∼7.[10]

Herein, we report the synthesis and single-crystal X-ray structure analyses of $(NH_4)_6Ni^{II}_{0.5}[\alpha\text{-}Fe^{III}O_4W_{11}O_{30}Ni^{II}O_5(OH_2)]\cdot 18H_2O$, $(NH_4)_7Zn_{0.5}[\alpha\text{-}ZnO_4W_{11}O_{30}ZnO_5(OH_2)]\cdot 18H_2O$, and $(NH_4)_7Ni^{II}_{0.5}[\alpha\text{-}ZnO_4W_{11}O_{30}Ni^{II}O_5(OH_2)]\cdot 18H_2O$. The compounds have been characterized in the solid state and solution by elemental and thermal analyses, UV−vis, IR, Raman, ESR, and ^1H and ^{183}W NMR spectroscopy. Furthermore, we present evidence that the 3d-metal-disubstituted Keggin anions do not exist in solution but are being formed during the crystallization process.

Experimental Section

Synthesis of the 1:11:1 Complexes NH_4-M(3d)W_{11}M′(3d). The synthesis of the 3d disubstituted 1:11:1 POTs is carried out by slow addition of the metal acetates to aqueous sodium tungstate solutions, which had been acidified to a pH of 6.5−7.0, thus adding metal salt solutions to a mixture of the paratungstates A or B. It therefore appeared reasonable to conclude that the 3d disubstituted 1:11:1 POTs might equally be obtained by either (1) starting with $Na_2WO_4\cdot 2H_2O$ and HCl, (2) using $Na_6[W_7O_{24}]\cdot\sim 14H_2O$ (paratungstate A), or (3) even utilizing $Na_{10}[H_2W_{12}O_{42}]\cdot\sim 27H_2O$ (paratungstate B) as starting material. All three routes have been carried out for $(NH_4)_6Ni^{II}_{0.5}[\alpha\text{-}Fe^{III}O_4W_{11}O_{30}Ni^{II}O_5(OH_2)]\cdot 18H_2O$ (**NH_4-$Fe^{III}W_{11}Ni^{II}$**), $(NH_4)_7Zn_{0.5}[\alpha\text{-}ZnO_4W_{11}O_{30}ZnO_5(OH_2)]\cdot 18H_2O$ (**NH_4-$ZnW_{11}Zn$**), and $(NH_4)_7Ni^{II}_{0.5}[\alpha\text{-}ZnO_4W_{11}O_{30}Ni^{II}O_5(OH_2)]\cdot 18H_2O$ (**NH_4-$ZnW_{11}Ni^{II}$**) and also for $(NH_4)_7Na[\alpha\text{-}Co^{II}O_4W_{11}O_{30}Co^{II}O_5(OH_2)]\cdot\sim 16H_2O$ (**NH_4-$Co^{II}W_{11}Co^{II}$**); hence, identical products[14] were obtained in all three preparations for the individual compounds. While the yields obtained with the two first routes are very similar (35−40%, based on the recovered, crystalline material), the yields obtained with $Na_{10}[H_2W_{12}O_{42}]\cdot\sim 27H_2O$ were below 20%. This can

(4) Baker, L. C. W.; Figgis, J. S. *J. Am. Chem. Soc.* **1970**, *92*, 3794−3797.
(5) (a) Tézé, A.; Hervé, G. *Inorg. Synth.* **1990**, *27*, 85−96. (b) Knoth, W. H.; Harlow. R. L. *J. Am. Chem. Soc.* **1981**, *103*, 1865−1867. (c) Domaille, P. J. *Inorg. Synth.* **1990**, *27*, 96−104.
(6) Hill, C. L. Polyoxometalates: Reactivity. In *Comprehensive Coordination Chemistry (II)*; McCleverty, J. A., Meyer, T. J., Eds.; Elsevier Ltd.: Oxford, UK, 2004; Vol. 4, 679−759. See pages 684−691 and refs 88−90, and 122−128 therein.
(7) The literature on multiple metal-substituted framework-incorporated polyoxoanions is extensive. A representative summary of 40 relevant references (Table S1) and further information on additional literature (Table S2) is provided in the Appendix of the Supporting Information.
(8) For references concerning synthesis and characterization of multiple metal-substituted (3A and 3d) polyoxometalates based on nona- and decatungstosilicates and -phosphates see: Wassermann, K.; Palm, R.; Lunk, H.-J.; Steinfeld, N.; Stösser, R. *Inorg. Chem.* **1995**, *34*, 5029−5036 and refs 5 and 6 therein.
(9) Previously classified as multiple metal-substituted framework-incorporated polyoxoanions, see: Weiner, H.; Hayashi, Y.; Finke, R. G. *Inorg. Chem.* **1999**, *38*, 2579−2591.
(10) Baker, L. C. W.; McCutcheon, T. P. *J. Am. Chem. Soc.* **1956**, *78*, 4503−4510.
(11) Barrett, A. S. *Diss. Abstr.* **1972**, *33B*, 1475-B.
(12) Thus far, no lacunary heteropoly tungstates with a *divalent* central heteroatom have been reported. The preparation of the lacunary $[Fe^{III}O_4W_{11}O_{35}]^{9-}$ is mentioned in: Zonnevijlle, F., Ph.D. Thesis, Université des Sciences et Techniques du Languedoc: Montpellier, France, 1976.
(13) (a) Bradley, J. S.; Patrick, V. A. *Aust. J. Chem.* **2002**, *55*, 281−286. (b) Bradley, J. S.; Patrick, V. A. *Aust. J. Chem.* **2000**, *53*, 965−970. (c) Cruywagen, J. J. *Adv. Inorg. Chem.* **2000**, *49*, 127−182. (d) Nolan, A. L.; Allen, C. C.; Burns, R. C.; Lawrance, G. A.; Wilkes, E. N.; Hambley, T. W. *Aust. J. Chem.* **1999**, *52*, 955−964. (e) Hastings, J. J.; Howarth, O. *J. Chem. Soc., Dalton Trans.* **1992**, 209−215.
(14) The products of the two alternative routes (starting from either paratungstate A or B) were compared to the general procedure (from Na_2WO_4) by their UV−vis, IR, Raman, and ESR (for **NH_4-$Fe^{III}W_{11}Ni^{II}$**) spectra.

be explained by the slow hydrolysis of aqueous solutions of $[H_2W_{12}O_{42}]^{10-}$ to $[W_7O_{24}]^{6-}$ at elevated temperatures.[15]

General Procedure—Starting with Sodium Orthotungstate. $Na_2WO_4 \cdot 2H_2O$ (20.0 g, 68.0 mmol) was dissolved in 100 mL of H_2O at room temperature (pH = 8.5). Glacial acetic acid was added dropwise with stirring over ca. 10 min to the tungstate solution to adjust the pH to 6.5 ± 0.1 (ca. 4 mL of acetic acid was used in this step). Separately, 18.52 mmol of anhydrous NaAc was dissolved in 50 mL of water. Then, the solution of a total of 12.36 mmol of the solid transition metal compounds (6.18 mmol each in case of the mixed metal complexes) in 50 mL of a 0.37 M sodium acetate solution was added dropwise to the tungstate solution under stirring over 2 h (ca. 0.5 mL/min), while the temperature was kept at ca. 80 °C during this time.

The tungstate solution remained clear and homogeneous upon addition of the metal salt solution; no precipitate should be formed at this stage. *Note: If a precipitate is formed, the addition of the metal salt solution should be stopped until all of the precipitate is redissolved.* After the addition of the metal salt solution was completed, the reaction solution was stirred for another 4−16 h at 80−85 °C. After cooling to 60−65 °C, 25.0 g (32.42 mmol, excess) of solid NH_4Ac was added to the warm solution in one single step under stirring. A precipitate was formed within 1 min. The mixture was then allowed to cool to room temperature in an ice bath and stirred for another 2 h at this temperature. The precipitate was then dissolved in 40 mL of acidified H_2O (prepared from 0.25 mL of glacial acetic acid and 250 mL of H_2O; pH = 3.3) at 60 °C and stirred for 30 min at this temperature. If large amounts of precipitate remained, it was filtered off and the extraction was repeated, collecting a total of 80 mL of a clear and homogeneous filtrate. The combined filtrates were allowed to cool to room temperature and then left for crystallization at 5 °C for 24−48 h to yield 5.3−16.8 g of crystalline material. The crude product was recrystallized from 70 to 75 °C H_2O (pH 3.3), using approximately 2.5−3.0 mL/g of crude product to yield 2.12−9.85 g of crystalline material.

NH_4-$Fe^{III}W_{11}Ni^{II}$. The compound was prepared, using 1.52 g (18.52 mmol) of anhydrous NaAc, 1.54 g (6.18 mmol) of $Ni(Ac)_2 \cdot 4H_2O$ and 1.67 g (6.18 mmol) of $FeCl_3 \cdot 6H_2O$. The crude material (ca. 5.8 g) was collected on a glass frit (medium) and recrystallized as described in the general procedure. Yield: 4.10 g (20.5% based on W) of green, cubic crystals.

NH_4-$ZnW_{11}Zn$. The compound was prepared, applying 1.52 g (18.52 mmol) of anhydrous NaAc and 3.68 g (12.36 mmol) of $Zn(NO_3)_2 \cdot 6H_2O$. The crude product (16.8 g) was collected on a 50 mL glass frit (medium) and recrystallized twice from 70 to 75 °C H_2O (pH 3.3) using 2.5 mL of H_2O per gram of crude product. Yield: 9.85 g (49.6% based on W) of colorless, crystalline material.

NH_4-$ZnW_{11}Ni^{II}$. The compound was prepared, using 1.52 g (18.52 mmol) of anhydrous NaAc, 1.54 g (6.18 mmol) of $Ni(Ac)_2 \cdot 4H_2O$, and 1.84 g (6.18 mmol) of $Zn(NO_3)_2 \cdot 6H_2O$. Approximately 11.3 g of crude product was obtained, which was recrystallized as described above. Yield: 5.12 g (25.8% based on W) of green, crystalline material.

Alternative Procedure A—Starting with Sodium Paratungstate A. NH_4-M(3d)W_{11}M′(3d) could also be prepared directly from sodium heptatungstate hydrate[16] as starting material. Sodium paratungstate A, $Na_6[W_7O_{24}] \cdot \sim 14H_2O$ (20.0 g, 9.70 mmol) was dissolved in 100 mL of H_2O under stirring while heating the mixture to 80−85 °C over 1 h. All other manipulations were carried out exactly as described above. Approximately 10.8 g of crude product **NH_4-$Fe^{III}W_{11}Ni^{II}$** was obtained with this procedure. It was recrystallized as described above to yield 5.82 g (29.2% based on W) of green, crystalline material. **NH_4-$ZnW_{11}Zn$** was prepared, working with 20.0 g (9.70 mmol) of $Na_6[W_7O_{24}] \cdot \sim 14H_2O$, 1.52 g (18.52 mmol) of anhydrous NaAc, and 3.68 g (12.36 mmol) of $Zn(NO_3)_2 \cdot 6H_2O$. The synthesis of **NH_4-$ZnW_{11}Ni^{II}$** was started with 20.0 g (9.70 mmol) of $Na_6[W_7O_{24}] \cdot \sim 14H_2O$, 1.52 g (18.52 mmol) of anhydrous NaAc, 1.54 g (6.18 mmol) of $Ni(Ac)_2 \cdot 4H_2O$, and 1.84 g (6.18 mmol) of $Zn(NO_3)_2 \cdot 6H_2O$. Approximately 10.8 g of crude product was obtained, which was recrystallized as described above. Yield: 5.20 g (26.3% based on W) of green, crystalline material.

The *alternative procedure A* was used for the preparation of the well-known analogous Co^{II} compound **NH_4-$Co^{II}W_{11}Co^{II}$**.[10] The compound was prepared, working with 20.0 g (9.70 mmol) of $Na_6[W_7O_{24}] \cdot \sim 14H_2O$ and 3.08 g (12.36 mmol) of $Co(Ac)_2 \cdot 4H_2O$. Approximately 6.88 g of crude product was obtained with this procedure, which was recrystallized four times as described for **NH_4-$Fe^{III}W_{11}Ni^{II}$**, vide supra. Yield: 2.12 g (10.6% based on W) of dark emerald-green, crystalline material.

Alternative Procedure B—Starting with Sodium Paratungstate B. The complexes **NH_4-$Fe^{III}W_{11}Ni^{II}$** and **NH_4-$ZnW_{11}Zn$** were prepared using sodium paratungstate B[17] as starting material. Solid $Na_{10}[H_2W_{12}O_{42}] \cdot \sim 27H_2O$ (20.48 g, 5.66 mmol) was dissolved in 100 mL of H_2O under stirring while heating the mixture to 80−85 °C over 1 h. Separately, 1.52 g (18.52 mmol) of anhydrous NaAc was dissolved in 50 mL of water. For the preparation of **NH_4-$Fe^{III}W_{11}Ni^{II}$**, 1.54 g (6.18 mmol) of solid $Ni(Ac)_2 \cdot 4H_2O$ was added to the solution of the sodium acetate, followed by the addition of 1.67 g (6.18 mmol) of solid $FeCl_3 \cdot 6H_2O$. For **NH_4-$ZnW_{11}Zn$**, 3.68 g (12.36 mmol) of solid $Zn(NO_3)_2 \cdot 6H_2O$ was added to the solution of the sodium acetate and dissolved under stirring. All other manipulations were carried out exactly as described above in the general procedure. Both compounds were authenticated by their UV−vis, IR, and Raman spectra.

Synthesis of Other M(3d)W_{11}M′(3d) Complexes. In addition to the four complexes described above in detail, mixed-metal 1:11:1 complexes with Zn/Fe^{III} (NH4-ZnW11FeIII) and Co^{II}/Ni^{II} (NH_4-$Co^{II}W_{11}Ni^{II}$) have been prepared. The syntheses follow closely the above-described general procedures; hence, more details are provided in the Supporting Information, pages 13−14, for the interested reader.

Elemental Analysis, Calcd (found)%. $H_{62}FeN_6Ni_{1.5}O_{58}W_{11}$. MW = 3240.7: Fe, 1.72 (2.18); NH_3, 3.15 (3.17); Ni, 2.72 (2.66); W, 62.40 (59.90); H_2O, 10.00 (8.98); Na, −(0.13). IR (400−1200 cm^{-1}, KBr pellet): 941(s), 878(s), 737(m), 759(m), 674(w), 662-(w), 534(w), 449(w). UV ($c = 1.63 \times 10^{-2}$ mM), λ/nm (ϵ(L(mol × cm)$^{-1}$): 257sh/3.0 × 10^4. Vis ($c = 0.013$ M), λ/nm (ϵ(L(mol × cm)$^{-1}$): 413/85; 468/19; 711/9; 463/4; 448/4.

$H_{66}N_7O_{58}W_{11}Zn_{2.5}$. MW = 3278.4: NH_3, 3.63 (3.49); W, 61.69 (60.2, 62.1); Zn, 4.99 (4.52, 4.77); H_2O, 10.44 (10.68), Na, -(0.09,

(15) After heating a 4.3×10^{-3} M solution of paratungstate B for 18 h at 80 °C, the amount of monotungstate and metatungstate was found to have declined in favor of the heptatungstate. After 120 h, the heptatungstate ion remains as the main species in solution. (a) Jander, G. *Z. Anorg. Allg. Chem.* **1951**, *265*, 244−254. (b) Stelzer, J. B. Ph.D. Thesis, Freie Universität, Berlin, Germany, 2000.

(16) Sodium heptatungstate hydrate, $Na_6[W_7O_{24}] \cdot \sim 14H_2O$ was prepared according to a known literature procedure;[15b] its identity was confirmed by IR spectroscopy. (a) Petrunkov, P. P.; Burtseva, K. G.; Semchenko, D. P. *Russ. J. Inorg. Chem.* **1976**, *21*, 1308−1310. (b) Burtseva, K. G.; Kochubei, L. A.; Voropanova, L. A.; Gorbatkova, B. Kh. *Russ. J. Inorg. Chem.* **1981**, *26*, 1143−1144.

(17) Sodium paratungstate hydrate, $Na_{10}[H_2W_{12}O_{42}] \cdot \sim 27H_2O$ (**Na-PT**, paratungstate B), was prepared according to a known literature procedure (Vallance, R. H. *J. Chem. Soc.* **1931**, 1421−1435). Its identity was confirmed by IR spectroscopy in comparison to the literature and by TGA.

0.09). IR (400−1200 cm^{-1}, KBr pellet): 934(s), 878(s), 752(m), 718(m), 661(w), 555(w), 546(w), 449(w). UV ($c = 4.08 \times 10^{-2}$ mM), λ/nm (ϵ(L(mol × cm)$^{-1}$): 257sh (2.6×10^4).

$H_{66}N_7Ni_{1.5}O_{58}W_{11}Zn$. MW = 3268.3: NH_3, 3.64 (3.31); Ni, 2.69 (2.44, 2.78); W, 61.88 (62.6, 61.5); Zn, 2.00 (1.97, 2.10); H_2O, 10.47 (11.96); Na, −(0.01, 0.01). IR (400−1200 cm^{-1}, KBr pellet): 941(s), 879(s), 797(m), 747(m), 662(w), 563(w), 547(w), 451(w). UV ($c = 2.95 \times 10^{-2}$ mM), λ/nm (ϵ/L(mol × cm)$^{-1}$): 257sh/2.8×10^4. Vis ($c = 0.023$ M), λ (ϵ/L(mol × cm)$^{-1}$): 428/14; 696/5.

Analytical and Instrumental Procedures. Nitrogen analysis was carried out by using the Kjeldahl method. Approximately 150 mg of solid was placed in a NaOH solution using a Kjeltec 1026 unit. The evolving NH_3 gas was trapped in a saturated boric acid solution and then titrated with 0.4 N HCl to determine the NH_3 content. Auto-titration was performed with a DL67 Mettler autotitrator. Elemental analysis of the metals (W, Fe, Co, Ni, Zn, and Na) was done by atomic absorption spectroscopy (AAS) using a Perkin-Elmer atomic absorption spectrometer PE 5100 PC.

TGA analyses (Mettler TGA/SDTA 851e with TSO800GC1 gas control box) were done under air over a temperature range of 18−700 °C (10 K/min). For determination of the amount of crystal water, intact, well-shaped crystals (0.3−1.5 mm; ∼30 mg) were removed from the mother liquids, placed on clay plates, and dried under argon at room temperature before being transferred into the crucibles (70 μL, α-Al_2O_3).

Single-crystal X-ray data were collected on a Bruker-XPS-diffractometer (CCD area detector, Mo Kα radiation, $\lambda = 0.71073$ Å, graphite monochromator at 172(2) K). Empirical absorption correction was done by means of symmetry-equivalent reflections (SADABS).[18a] The structures were solved by the direct methods SHELXS-97[18b] and refined using the full-matrix least squares and difference Fourier methods of the program SHELXL-97[18c] in the WINGX system.[18d] No hydrogen atoms could be located. All of the non-hydrogen atoms were refined anisotropically. The nitrogen atoms in NH_4^+ and oxygen in H_2O were crystallographically distinguished by their chemical surroundings in the crystal structure as plausibly as possible. Supplementary crystallographic material for **NH_4-$Fe^{III}W_{11}Ni^{II}$**, **NH_4-$ZnW_{11}Zn$**, and **NH_4-$ZnW_{11}Ni^{II}$** in CIF format is available as Supporting Information.

^{1}H NMR (300.15 MHz) spectra were recorded in 5-mm o.d. tubes on a Bruker AC-300 NMR spectrometer at 21 °C and were referenced to the residual impurity in the deuterated solvent. Spectral parameters for ^{1}H NMR include ^{1}H pulse width, 3.0 ms; acquisition time, 1.360 s; repetition rate, 2.35 s; and sweep width, ±6024 Hz. ^{183}W NMR (20.8 MHz) spectra were recorded on a Bruker AM-500 NMR spectrometer in 10-mm o.d. NMR tubes at 21 °C and referenced to saturated Na_2WO_4/D_2O by the external substitution method. Acquisition parameters were as follows. ^{183}W pulse width, 30 μs; acquisition time, 1.114 s; relaxation delay, 1.000 s, and sweep width, ±14705 Hz. An exponential line-broadening apodization (5 Hz) was applied to all spectra but was removed for any line widths reported herein. The chemical shifts are reported on the δ scale with downfield resonances as positive. All manipulations were carried out under air and at 1 atm pressure.

The ^{1}H solid-state NMR experiments were carried out on a Varian/Chemagnetics CMX-360 spectrometer using a Doty XC5 5-mm double-resonance magic angle spinning (MAS) probe. The ^{1}H resonance frequencies were 360.24 MHz, and the magic-angle spinning rates were set as 10 kHz. The samples were packed into the 5-mm rotors in a glovebag with flowing nitrogen and were kept in the nitrogen atmosphere during the NMR experiments. A single pulse sequence with spectral width of 200 kHz, recycle delay of 11 s, and 256 scans was used to acquire the ^{1}H-MAS NMR spectra. The ^{1}H chemical shifts were referenced relative to TMS using a secondary external standard made of silicon rubber.

Electron spin resonance (ESR) spectra were collected at the West Virginia University in the Department of Chemistry. The spectra were collected on a Bruker electron paramagnetic resonance spectrometer, model B-E2549, with a 10-in. magnet equipped with a built-in microwave frequency meter. The spectrometer was operated by means of a Bruker EMX-A control system. The WIN-EPR software package was used for data analysis.

IR spectra (400−4000 cm^{-1}; Genesis Series FTIR, Mattson) were obtained as KBr disks. KBr (Aldrich, spectrophotometric grade) was used as received. All samples were dried under vacuum at 120 °C for 24 h prior to the preparation of the KBr disks. Raman spectra (100−1200 cm^{-1}) were collected using a Kaiser Raman system at 532 nm (solids, 4 s, 10 repeats; liquids, 10 s, 10 repeats).

The UV−vis spectra were recorded using a HP 845A diode-array system interfaced to an IBM 486 computer. The UV spectra were recorded using aqueous solutions (0.015−0.052 mM) of the POTs; spectra for the visible region were collected using 5.5×10^{-3}−0.1 M aqueous solutions.

Results and Discussion

Solid State Characterization. Elemental Analysis. The molecular formulas of the four POTs **NH_4-$Fe^{III}W_{11}Ni^{II}$**, **NH_4-$ZnW_{11}Zn$**, **NH_4-$ZnW_{11}Ni^{II}$**, and **NH_4-$Co^{II}W_{11}Co^{II}$** were established by elemental analyses (all elements and Na, except oxygen; see the Experimental Section). Nitrogen analyses require the formulation of heptakis(ammonium) salts for **NH_4-$ZnW_{11}Zn$** and **NH_4-$ZnW_{11}Ni^{II}$** and a hexakis-(ammonium) salt for **NH_4-$Fe^{III}W_{11}Ni^{II}$**. Sodium analyses confirmed the absence of Na^+ in **NH_4-$Fe^{III}W_{11}Ni^{II}$**, **NH_4-$ZnW_{11}Zn$**, and **NH_4-$ZnW_{11}Ni^{II}$** but require the formulation of a heptakis(ammonium) monosodium salt for **NH_4-$Co^{II}W_{11}Co^{II}$**. Thermal analyses, carried out under air and nitrogen, confirmed the presence of 16−18 mol of crystal water in the ammonium salts of the 1:11:1 POTs. A summary of analysis data and calculated elemental compositions is provided in the Supporting Information, Table S3.

X-Ray Single-Crystal Structure Analyses. The three POTs **NH_4-$Fe^{III}W_{11}Ni^{II}$**, **NH_4-$ZnW_{11}Zn$**, and **NH_4-$ZnW_{11}Ni^{II}$**, crystallize in the cubic system. The crystal structures were solved and refined in the space group $Fm\bar{3}m$ to R values of 2.66, 2.12, and 2.38%, respectively. All attempts to refine the crystal structures in a space group of lower symmetry were unsuccessful. The solid-state structures of the three compounds consist of four main structural fragments, namely $[MO_4W_{11}O_{30}M'O_5(OH_2)]^{n-}$ (Keggin-type, α-isomer) POTs, **a**; hexaquo metal cations, $[M''(OH_2)_6]^{2+}$, **b**, ammonium−water cluster ions, $[(NH_4^+)_8(OH_2)_{12}]$, **c**, and additional ammonium cations and water molecules, **d**. The 3d metals were found to be distributed over three different positions: the central (tetrahedral) position (M), the peripheral (octahedral) positions of the Keggin anion (M′), and cationic positions (M″) outside of the POT framework (see Figure 2).

(18) (a) *Area-Detector Absorption Correction*; Siemens Industrial Automation, Inc.: Madison, WI, 1996. (b) Sheldrick, G. M. *Acta Crystallogr.* **1990**, *A46*, 467−473. (c) Sheldrick, G. M., University of Göttingen, Germany, 1997. (d) Farrugia, L. J. *J. Appl. Crystallogr.* **1999**, *32*, 837−838.

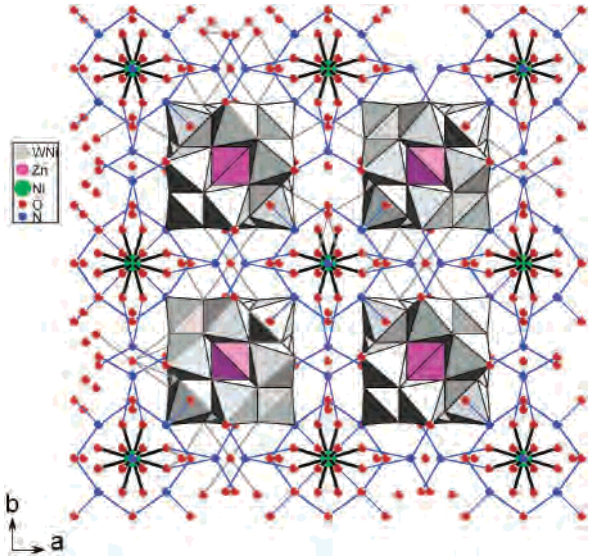

Figure 2. X-ray crystal structure of $(NH_4)_7Ni^{II}_{0.5}[\alpha\text{-}ZnO_4W_{11}O_{30}Ni^{II}O_5(OH_2)]\cdot\sim 18H_2O$ showing the main structural fragments: Keggin-type heteropolytungstate, (α-isomer, in polyhedral representation), $[Ni^{II}(OH_2)_6]^{2+}$, and $[(NH_4^+)_8(OH_2)_{12}]$. The 3d metals are distributed over three different positions, the central position (Zn^{II}) and the peripheral positions of the Keggin anion (W^{VI}, Ni^{II}), and cationic positions (Ni^{II}) outside of the polyoxotungstate framework.

One of the 12 octahedrally coordinated W atoms is substituted statistically by one of the 3d metal cations M′, and the corresponding terminal oxygen atom is replaced by an H_2O ligand. The occupational parameters for M′ varied over the refinement and the analysis of independent samples from 0.9 to 1.1. The four hexaquo metal cations, $[M''(OH_2)_6]^{2+}$, **b**, per unit cell are disordered. In **NH_4-$ZnW_{11}Zn$**, all three 3d metal positions (M, M′, and M″) are occupied by Zn^{II}. A distinction between the 3d metal cations occupying the central (M) and the peripheral (M′) position in **$ZnW_{11}Ni^{II}$** can be made by comparing the 3d metal−oxygen bond lengths. The M−O bond lengths of the central $\{MO_4\}$ tetrahedron in **$ZnW_{11}Zn$** and **$ZnW_{11}Ni^{II}$** with 1.914(7) and 1.907(7) Å are nearly identical and in good agreement with the Zn−O distance (1.976 Å) in ZnO.[19a] Hence, it can be concluded that the central (tetrahedral) position in *both* **$ZnW_{11}Zn$** and **$ZnW_{11}Ni^{II}$** is occupied by Zn^{2+}. (Note: The Ni−O bond length determined for tetrahedrally oxygen coordinated Ni^{II} in $NiAl_2O_4$ with 1.80 Å is significantly shorter.[19b]) In **NH_4-$ZnW_{11}Ni^{II}$**, Ni^{II} is therefore distributed over the peripheral (M′) and the cationic (M″) positions. A distinction between the positions for the 3d metal ions in **NH_4-$Fe^{III}W_{11}Ni^{II}$**, however, proved considerably more difficult. The M−O bond length was 1.84 Å for the central $\{MO_4\}$ tetrahedron, which ranges between values for Ni^{II} and Fe^{III}, tetradedrally coordinated by oxygen, previously reported for $NiAl_2O_4$ and Fe_3O_4, respectively.[19b,20] Incidentally, the same average M−O distance of 1.84 Å was found for $\{Fe^{III}O_4\}$ in **Ba-$Fe^{III}W_{12}$**, and the occupation of the central tetrahedron by Fe^{III} was verified by ESR spectroscopy (see Figure 4 of this work, also ref 21). A comparison of the

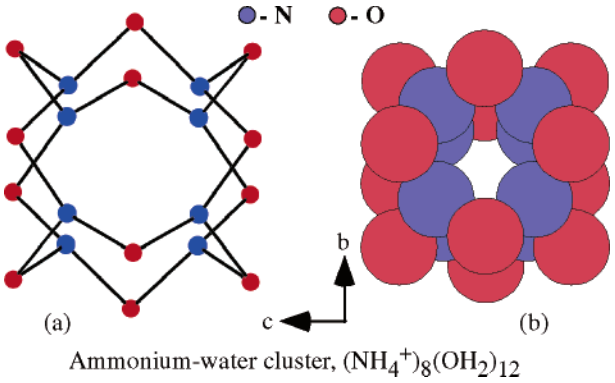

Figure 3. Ball-and-stick and space-filling models of the ammonium−water cluster ion $[(NH_4^+)_8(OH_2)_{12}]$.

ESR spectra of **NH_4-$Fe^{III}W_{11}Ni^{II}$**, **K-$SiW_{11}Fe^{III}$**, and **Ba-$Fe^{III}W_{12}$**, revealed that Fe^{III} in **$Fe^{III}W_{11}Ni^{II}$** occupies the tetrahedral position ($g' \approx 6$). It can therefore be concluded, that Ni^{II} in crystalline **NH_4-$Fe^{III}W_{11}Ni^{II}$**, is distributed over the peripheral, octahedral (M′), and the cationic positions (M″). The octahedrally coordinated H_2O ligands of the 3d hexaquo complexes $[M''(OH_2)_6]^{2+}$, **b**, are 4-fold disordered. The arrangement of the structural fragments **a**, **b**, and **c** can best be described with a filled CaF_2 structure in which the centers of the POTs, **a**, are occupying the F^- positions and the 3d hexaquo metal complexes, **b**, are located at the Ca^{2+} positions. The $[(NH_4^+)_8(OH_2)_{12}]$ clusters, **c**, are placed in the remaining cubic vacancies. In the three structures, the 12 edges of a NH_4^+ cube are connected to H_2O through hydrogen bonding, resembling a perhomocuban-like structure (see Figure 3).[22] The residual ammonium cations and water molecules, **d**, occupy the interstices and are connected to **a**, **b**, and **c** through strong hydrogen bonding.

The nitrogen atoms in NH_4^+ and oxygen in H_2O were crystallographically distinguished by their chemical surroundings in the crystal structure as plausibly as possible. The size and shape of the H_2O clusters depend on appearance and symmetry of the vacancies within the crystal lattice. Even more complex H_2O clusters have recently been reported by Müller et al. for polyoxomolybdate-based porous "nano containers".[23]

Only minor differences were observed in the lattice parameters for **NH_4-$Fe^{III}W_{11}Ni^{II}$**, **NH_4-$ZnW_{11}Zn$**, and **NH_4-$ZnW_{11}Ni^{II}$**. A summary of crystallographic data, in-

(19) (a) Schulz, H.; Thiemann, H. *Solid State Commun.* **1979**, *32*, 783−785. (b) Furuhashi, H.; Inagaki, M.; Naka, S. *J. Inorg. Nucl. Chem.* **1973**, *35*, 3009−3014.

(20) Various studies on composition and structure of Fe_3O_4 in dependence of temperature and pressure have been carried out. (a) Fleet, M. E. *J. Solid State Chem.* **1986**, *62*, 75−82; disordered, octahedral $Fe^{II/III}$−O, 2.059 Å, tetrahedral Fe^{II}−O, 1.891 Å. See also: (b) Escobar, C.; Cid-Dresdner, H.; Kittl, P.; Duemler, I. *Am. Mineral.* **1971**, *56*, 489−498; $FeWO_4$ (Ferberit), Fe^{II}−O, 2.003, 2.072, 2.170 Å (each 2×). (c) Pinto, H.; Memalud, M.; Shaked, H. *Acta Crystallogr. A* **1977**, *33*, 663−667; Neutron scattering of Fe_2WO_6 (Magnetit), Fe^{III}−O, 1.955, 1.986, 2.081 Å (each 2×); Fe^{III}−O, 1.819, 2.048, 2.156 Å (each 2×).

(21) (a) Weiner, H.; Lunk, H.-J.; Stösser, R.; Lück, R. *Z. Anorg. Allg. Chem.* **1989**, *572*, 164−174. (b) Pietzsch, C.; Weiner, H.; Schönherr, S.; Lunk, H.-J.; Stösser, R. *Isotopenpraxis* **1991**, *27*, 65−68.

(22) Zefirov, N. S.; Palyulin, V. A.; Samoshin, V. V.; Svyatkin, V. A.; Trach, S. S. *J. Org. Chem. USSR* **1987**, *23*, 302−305.

(23) Müller, A.; Krickemeyer, E.; Bögge, H: Schmidtmann, M.; Botar, B.; Talismanova, M. O. *Angew. Chem., Int. Ed.* **2003**, *42*, 2085−2090.

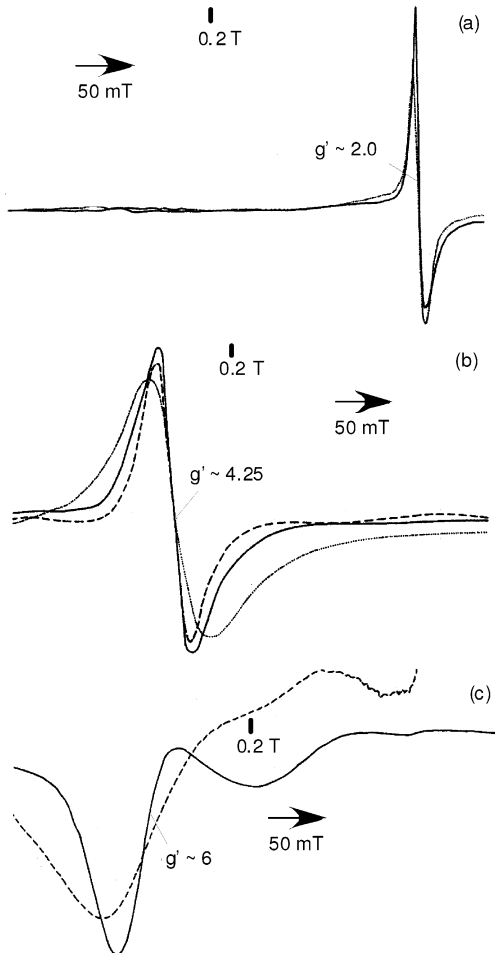

Figure 4. ESR spectra of heteropolytungstates containing Fe^{III} in tetrahedral and octahedral coordination. (a) *tetrahedral*: $Ba-Fe^{III}W_{12}$ at 298 (·····) and 77 K (—); (b) *octahedral*: $K-SiW_{11}Fe^{III}$ at 298 (·····), 77 (—), frozen aqueous solution at 77 K; (c) *tetrahedral*: $NH_4-Fe^{III}W_{11}Ni^{II}$ at 298 (·····) and 77 K (—).

cluding relevant bond lengths and angles is provided in Tables 1 and 2.

NMR Spectroscopy (See also NMR Spectroscopy in the Studies of Aqueous Solutions section). Whereas the observation of the nonexchanging protons in aqueous solutions of metatungstate confirms the presence of structurally intact $[(H_2O_4)W_{12}O_{36}]^{6-}$ Keggin units, the two nonacid protons in paratungstate B are exchanging rapidly with the solvent and can only be observed in the solid, polycrystalline materials.[24] ^{1}H-MAS NMR spectroscopy (rotation frequency, 10 kHz) was carried out comparing **K-ZnW$_{11}$Zn** (synthesized by the general procedure, but using KAc instead of NH_4Ac), **K-MT**,[24b] and **K-PT**[25] in the solid state. By using the potassium, rather than the ammonium salts of the POTs, a distinction between the protons of water molecules and the nonacidic protons in paratungstates can be made. For **K-MT**, the two nonacidic protons are characterized by a signal at 6.4 ppm. The data obtained for **K-PT** are in agreement with previous studies,[25] indicating the presence of hydrate water (4.2 ppm) and a signal at 5.7 ppm, which is indicative of the two nonacidic protons in solid $K_{10}[H_2W_{12}O_{42}]\cdot\sim 10H_2O$. The ^{1}H-MAS NMR spectrum of **K-ZnW$_{11}$Zn** shows the main signal at 4.1 ppm, which is assigned to the hydrate water. A small signal at 5.6 ppm indicates the presence of nonacidic protons from a paratungstate B impurity. However, the spectrum did not provide any indication of nonacidic protons stemming from metatungstate. The ^{1}H-MAS NMR spectra of **K-MT**, **K-PT**, and **K-ZnW$_{11}$Zn** are shown in Figure S4 of the Supporting Information.

ESR Spectroscopy. ESR spectroscopy of **NH_4-Fe^{III}W$_{11}$Ni^{II}** in comparison to **Ba-Fe^{III}W$_{12}$** and **K-SiW$_{11}$Fe^{III}** was carried out to obtain information about site symmetry and electronic structure of Fe^{III} in the **M(3d)W$_{11}$M′(3d)** POT. For **Ba-Fe^{III}W$_{12}$**, containing Fe^{III} in a tetrahedral coordination, a signal at $g' \approx 2$ with a line width, ΔB, of 4.8 mT was observed for the single crystal and is also seen for a polycrystalline material, Figure 4a. The signal is mainly caused by the $^1/_2 \leftrightarrow {}^1/_2$ fine structure transition in Fe^{III} and does show a significant anisotropy. The characteristic signal is also observed in a frozen aqueous solution, indicating that the $[Fe^{III}O_4W_{12}O_{36}]^{5-}$ Keggin anion in **Ba-Fe^{III}W$_{12}$** remains structurally intact in solution. The line broadening decreases at 77 K, and the signals for both the polycrystalline material and the frozen aqueous solution are nearly identical. A signal at $g' \approx 4.25$ with a ΔB of $\sim$ 26.5 mT is caused by Fe^{III}, situated in a rhombohedrally distorted octahedral coordination,[26] which is characteristic for **K-SiW$_{11}$Fe^{III}**, Figure 4b.

The ESR spectrum of **NH_4-Fe^{III}W$_{11}$Ni^{II}** at 298 K is characterized by a relatively broad signal at $g' \approx 6$, Figure 4c. This signal position is characteristic for ESR X-band spectra of Fe^{III} species in tetrahedral coordination undergoing a strong axial distortion caused, e.g., by another paramagnetic ion. By spin exchange, this ion (here Ni^{II}) then causes a temperature-dependent line-broadening effect accompanied by a slight signal shift. The line broadening decreases significantly at 77 K, indicating exchange interaction between the Fe^{III} ions and a second paramagnetic center (Ni^{II}). The interaction causes an averaging of parts of the Fe^{III} fine structure, locally resulting in a strong axial distortion of the electronic environment of the Fe^{III} ions. In comparison to other Fe^{III} complexes (i.e., iron(III) tetraphenylporphine, tetrabromoferrate(III)[27]) this indicates, but does not conclusively prove, a tetrahedral coordination for iron(III) in **NH_4-Fe^{III}W$_{11}$Ni^{II}**.

IR Spectroscopy. Infrared measurements for **NH_4-Fe^{III}W$_{11}$Ni^{II}**, **NH_4-ZnW$_{11}$Zn**, **NH_4-ZnW$_{11}$Ni^{II}**, and **NH_4-Co^{II}W$_{11}$Co^{II}**, Figure 5, suggest the presence of the Keggin-type $[MO_4W_{12}O_{36}]^{n-}$ POT in the solid state and

(24) The two central, nonexchanging protons in metatungstate are observed at ~1.5 ppm with respect to solvent water. (a) Pope, M. T.; Varga, G. M., Jr. *J. Chem. Soc., Chem. Commun.* **1966**, 653−654. (b) Lunk, H.-J.; Chuvaev, V. F.; Kolli, I. D.; Spitsyn, V. I. *Dokl. Akad. Nauk* **1968**, *181*, 357−360. Subsequent broadline NMR studies of solid metatungstates show $r_{H-H} = 1.92 \pm 0.03$ Å. Chuvaev, V. F.; Lunk, H.-J.; Spitsyn, V. I. *Dokl. Akad. Nauk* **1968**, *180*, 133−136.

(25) Fait, M.; Heidemann, D.; Lunk, H.-J. *Z. Anorg. Allg. Chem.* **1999**, *625*, 530−538.

(26) Blumberg, W. E. In *Magnetic Resonance in Biological Systems*; Ehrenberg, A., Malström, B. E., Vänngart, T., Eds.; Pergamon Press: London, UK, 1967; p 111.

(27) Feist, M.; Mehner, H.; Stösser, R.; Scholz, G.; Dwelk, H.; Kemnitz, E. *Solid State Sci.* **2002**, *4*, 109−115.

Table 1. Crystal Data and Structure Refinements

identification code	NH_4-$Fe^{III}W_{11}Ni^{II}$	NH_4-$ZnW_{11}Zn$	NH_4-$ZnW_{11}Ni^{II}$
empirical formula	$H_{62}FeN_7Ni_{1.50}O_{58}W$	$H_{57}N_7O_{58}W_{11}Zn_{2.50}$	$H_{62}N_7Ni_{1.5}O_{58}W_{11}Zn$
fw, g/mol^{-1}	3240.6	3278.3	3268.2
T, K	172(2)	172(2)	172(2)
λ, Å	0.71073	0.71073	0.71073
cryst syst/space group	cubic/$Fm\bar{3}m$	cubic/$Fm\bar{3}m$	cubic/$Fm\bar{3}m$
a, Å	22.406(3)	22.437(2)	22.372(2)
V, Å^3	11248(2)	11295(2)	11197(2)
Z, calcd. density d, g/cm^3	8, 3.844	8, 3.845	8, 3.873
μ, mm^{-1}	23.257	23.465	23.533
eff. transmission min/max	0.420	0.406	0.348
F_{000}	11656	11667	11683
cryst dimensions, mm	0.24 × 0.15 × 0.07	0.5 × 0.35 × 0.22	0.19 × 0.19 × 0.07
Θ, (deg)	2.57−27.51	3.01−30.52	2.58−30.47
limiting indices	$-29 \le h \le 28$	$-32 \le h \le 28$	$-31 \le h \le 29$
	$-32 \le k \le 29$	$-32 \le k \le 32$	$-30 \le k \le 31$
	$-29 \le l \le 29$	$-32 \le l \le 32$	$-31 \le l \le 31$
reflns collected/unique	28 564/709	34 979/922	35 229/917
	(R_{int} = 0.0693)	(R_{int} = 0.0569)	(R_{int} = 0.0593)
completeness of data, %	99.6	99.2	99.6
refinement method		full-matrix least-squares on F^2	
data/restraints/params	709/0/55	922/0/55	917/0/54
GOF on F^2	1.143	1.251	1.348
R_{final}, $I > 2\sigma(I)$	R1 = 0.0266	R1 = 0.0212	R1 = 0.0238
	wR2 = 0.0731	wR2 = 0.0490	wR2 = 0.0582
R (all data)	R1 = 0.0296	R1 = 0.0248	R1 = 0.0259
	wR2 = 0.0744	wR2 = 0.0509	wR2 = 0.0592
extinction coeff.	0.000014(2)	0.0000058(7)	
max., min. in final diff. map, e Å^{-3}	+1.463, −2.186	+1.325, −1.493	+1.258, −1.136

Table 2. Selected Bond Lengths (Å) for **NH_4-$Fe^{III}W_{11}Ni^{II}$**, **NH_4-$ZnW_{11}Zn$**, and **NH_4-$ZnW_{11}Ni^{II}$** (M = central metal, M′ = Peripheral Metal, M″ = Hexaquo Cation)

	$NH_4-Fe^{III}W_{11}Ni^{II}$ M, M′, M″ = Zn	$NH_4-ZnW_{11}Zn$ M = Zn; M′, M″ = Ni^{II}	$NH_4-ZnW_{11}Ni^{II}$ M = Fe^{III}; M′, M″ = Ni^{II}
W/M′−O(1)	2.210(5)	2.1555(3)	2.151(3)
W−O(2)	1.951(3)	1.972(3)	1.967(3)
W−O(3)	1.918(2)	1.924(2)	1.919(2)
W−O(4)	1.736(7)	1.744(5)	1.749(5)
M−O(1)	1.836(10)	1.914(7)	1.907(7)
M″(2)−O(20)	2.07(3)	2.10(2)	2.06(2)

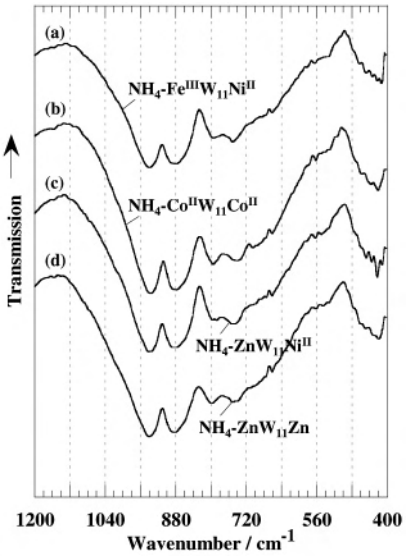

Figure 5. IR spectra of 3d-disubstituted polyoxotungstates (ammonium salts). (a) **NH_4-$Fe^{III}W_{11}Ni^{II}$**; (b) **NH_4-$Co^{II}W_{11}Co^{II}$**; (c) **NH_4-$ZnW_{11}Ni^{II}$**; (d) **NH_4-$ZnW_{11}Zn$**.

closely resemble those reported for the $XW_{11}Y$ (X = Si, P; Y = 3d, 3A) analogues.[28] Systematic vibrational studies of POTs relating to the Keggin structure have been reported previously.[29] In comparison with the α-XW_{12} Keggin anions (X = Si, P), additional bands are observed for the 3d-disubstituted POTs in the W−O spectral region (1000−760 cm^{-1}),[30] suggesting a lower symmetry for the M(3d)W_{11}M′-(3d) complexes.

Studies of Aqueous Solutions. The first step in the synthesis of iso- and heteropolytungstates in aqueous solution usually requires the acidification of sodium monotungstate, Na_2WO_4. Numerous studies on the reactions in aqueous tungstate solutions have been reported, addressing the complexity of equilibria and the kinetics involved.[1,13b] For example, paratungstate A, $[W_7O_{24}]^{6-}$, is formed rapidly (10^{-2} s at 10^{-4} M)[13b] upon acidification of aqueous solutions of WO_4^{2-}. The isomerization to the dodecameric paratungstate B, $[H_2W_{12}O_{42}]$,$^{10-}$ occurs over a period of several days, and the corresponding sodium salt, $Na_{10}[H_2W_{12}O_{42}]\cdot\sim 27H_2O$, crystallizes (at or below room temperature) from its solutions.

(28) (a) Peacock, R. D.; Weakley, T. J. R. *J. Chem. Soc. A* **1971**, 1836−1839. (b) Zonneville, F.; Tourné, C. M.; Tourné, G. F. *Inorg. Chem.* **1982**, *21*, 2742−2750.

(29) Rocchiccioli-Deltcheff, C.; Fournier, M.; Franck, R.; Thouvenot, R. *Inorg. Chem.* **1983**, *22*, 207−216. For systematic vibrational studies and important assignments of the spectra, see refs 11−13 therein.

(30) The symmetric and asymmetric stretchings of the M−O bonds (M = W, Mo) are observed in the following regions: M−O_t (*terminal* oxygens), 1000−960 cm^{-1}; M−O_c−M bridges between *corner*-sharing octahedra, 890−850 cm^{-1}; M−O_e−M bridges between *edge*-sharing octahedra, 800−760 cm^{-1}.

A stable equilibrium between paratungstate A and B is formed slowly over a time frame of several weeks, and a slight change of acidity appears to be required.[31] Heating of aqueous solutions of paratungstate B results in a quantitative conversion into paratungstate A. The reverse reaction, however, was found to be slow and did not proceed to completion.[15b] Consequently, paratungstate B only exists in freshly prepared solutions of the crystalline material; hence, recrystallization upon heating or the presence of other metal ions (i.e., 3d) result in the formation of mixtures of iso- and heteropolytungstates with varying compositions.[15b]

NMR Spectroscopy. A concern during the synthesis of the $M(3d)W_{11}M'(3d)$ complexes is the contamination of the final material with metatungstate (MT), $[(H_2O_4)W_{12}O_{36}]^{6-}$, in which the central tetrahedral position is occupied by two nonacid protons. Although less likely over the course of the general procedure (i.e., starting from Na_2WO_4 and H^+ at pH ≈ 7.0[32]) the synthesis route starting from sodium paratungstate B, $Na_{10}[H_2W_{12}O_{42}]\cdot\sim 27H_2O$, may give rise to the formation of some metatungstate due to its dismutation in hot, aqueous solution.[15] The presence of metatungstate containing two nonexchanging protons can be detected by ^{1}H NMR spectroscopy using sodium trimethyl acetate, $(CH_3)_3CCO_2^-Na^+$, as an internal standard.[33] No signals indicating the presence of nonexchanging protons on the NMR time scale were found for **NH_4-ZnW_{11}Zn** and **Na-PT** in comparison to **Na-MT**.

^{183}W NMR spectroscopy can provide valuable information about individual polytungstate species in complex mixtures in aqueous solutions.[34] The ^{183}W NMR spectrum for a structurally intact "$[\alpha$-$ZnO_4W_{11}O_{35}Zn(OH_2)]^{8-}$" Keggin anion should closely resemble that of the $[\alpha$-$XO_4W_{11}O_{35}]^{n-}$ (X = Si, P) "defect" Keggin anions.[35] The ^{183}W NMR spectra of the lacunary anions are characterized by six lines with intensity ratios 2:2:2:2:2:1, indicating that one W atom and its unshared O atom have been removed from the parent $[\alpha$-$XO_4W_{12}O_{36}]^{n-}$ (X = Si, P) Keggin structure.[35] The ^{183}W NMR spectrum of aqueous **NH_4-ZnW_{11}Zn**, however, appears very similar to that of sodium paratungstate B, showing the characteristic lines for both $[W_7O_{24}]^{6-}$ and $[H_2W_{12}O_{42}]^{10-}$,[36] rather than those for the XW_{11} lacunary structure. Apparently, a structurally intact Keggin anion is not retained upon redissolving the solid **NH_4-ZnW_{11}Zn** complex. Experimental details and the corresponding ^{1}H NMR and ^{183}W NMR spectra are provided in Figure S5 and Table S5-1, as well as in Table S6 and Figure S6-1, of the Supporting Information.

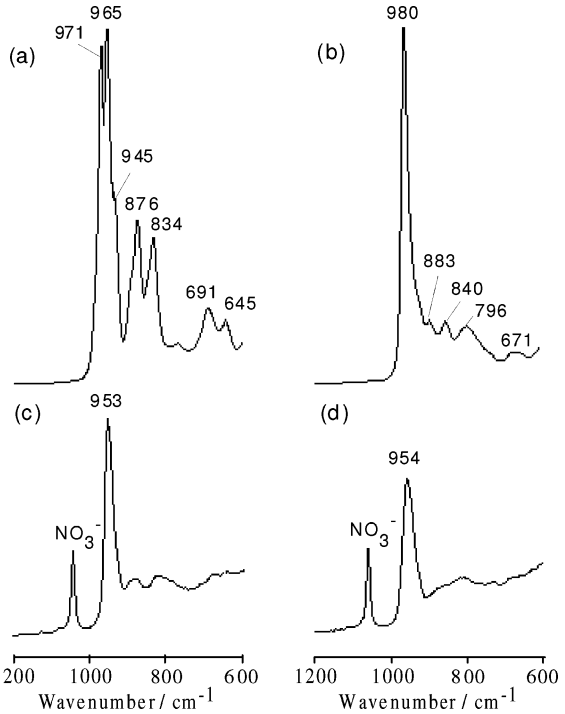

Figure 6. Raman spectra of $Na_6[W_7O_{24}]\cdot\sim 14H_2O$ and **NH_4-ZnW_{11}Zn**. (a) Solid $Na_6[W_7O_{24}]\cdot\sim 14H_2O$ (sodium paratungstate A); (b) solid **NH_4-ZnW_{11}Zn**; (c) aqueous solution (0.49 M in W) of $Na_6[W_7O_{24}]\cdot\sim 14H_2O$; (d) aqueous solution (0.50 M in W) of **NH_4-ZnW_{11}Zn**. Solid $NaNO_3$ was added to the aqueous solutions of (c) and (d) as an internal standard.

Raman Spectroscopy. Previous investigations[15b] have shown that the Raman solution and solid spectra of paratungstate A are nearly identical, confirming the existence of $[W_7O_{24}]^{6-}$ anions in solution and in the solid state. A comparison of Raman solution spectra for **NH_4-ZnW_{11}Zn** and paratungstate A is shown in Figure 6. The similarity between the spectra provides strong evidence for the existence of heptatungstate in the aqueous solutions of *both* materials.

UV−Vis Spectroscopy. UV spectra of Keggin-type POTs are characterized by an intense absorption around $(30-50) \times 10^3$ cm^{-1} with a maximum at approximately 38×10^3 cm^{-1} (263 nm) and a molar extinction coefficient (ϵ) of 10^4-10^5 L(mol·cm)$^{-1}$. The large band is due to the W ← O charge-transfer transition within the tungstate lattice and is commonly observed in the spectra of Keggin-type POTs with both central nonmetals and transition metals and also for metatungstate. The W ← O charge-transfer, observed as one broad absorption, has been found to be composed of several transitions and to be strongly influenced by the central metal

(31) Duncan, J. F.; Kepert, D. L. *J. Chem. Soc.* **1962**, 205−214.

(32) The formation of metatungstate occurs readily at pH < 5 and is a competing pathway during the synthesis of transition (and main group) metal XW_{12} complexes (X = Cu^{II}, Zn^{II}, Co^{II}, Fe^{III}, Al^{III}). This is a particular concern during the synthesis of heteropolytungstates containing M^{2+} which results in the formation of Keggin anions with identical charge (6−), and the purification of the final products can be tedious. (a) Mair, J. A. *J. Chem. Soc.* **1950**, 2364−2372. (b) Lunk, H.-J.; Giese, S.; Fuchs, J.; Stösser, R. *Z. Anorg. Allg. Chem.* **1993**, *619*, 961−968.

(33) The two central, nonexchanging protons in metatungstate are observed at ~1.5 ppm with respect to solvent water. (a) Pope, M. T.; Varga, G. M., Jr. *J. Chem. Soc., Chem. Commun.* **1966**, 653−654. (b) Lunk, H.-J.; Chuvaev, V. F.; Kolli, I. D.; Spitsyn, V. I. *Dokl. Akad. Nauk* **1968**, *181*, 357−360. Subsequent broadline NMR studies of solid metatungstates show $r_{H-H} = 1.92 \pm 0.03$ Å. Chuvaev, V. F.; Lunk, H.-J.; Spitsyn, V. I. *Dokl. Akad. Nauk* **1968**, *180*, 133−136.

(34) (a) Acerete, R.; Hammer, C. F.; Baker, L. C. W. *J. Am. Chem. Soc.* **1979**, *101*, 267−269. (b) Acerete, R.; Hammer, C. F.; Baker, L. C. W. *J. Chem. Soc.* **1982**, *104*, 5384−5390.

(35) Note that the characteristic six-line spectrum is still observed upon "completion" of the lacunary structure, i.e., for $[PW_{11}O_{40}Ti]^{5-}$ and $[PW_{11}O_{40}TiCl]^{4-}$. Knoth, W. H.; Domaille, P. J.; Roe, D. C. *Inorg. Chem.* **1983**, *22*, 198−201. See also: Gansow, O. A.; Ho, R. K. C.; Klemperer, W. G. *J. Organomet. Chem.* **1980**, *187*, C27−31 (α-[η^5-$C_5H_5Ti(PW_{11}O_{39})]^{4-}$).

(36) Maksimovskaya, R. I.; Burtseva, K. G. *Polyhedron* **1985**, *4*, 1559−1562.

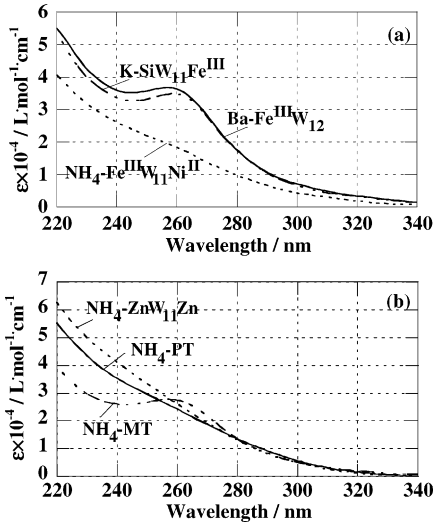

Figure 7. UV spectra of **NH_4-$Fe^{III}W_{11}Ni^{II}$**, **K-$SiW_{11}Fe^{III}$**, and **Ba-$Fe^{III}W_{12}$** in aqueous solution ($c \approx 1.6 \times 10^{-5}$ mol/L), (a). Characteristic maxima (λ_{max}) were observed for **K-$SiW_{11}Fe^{III}$** and **Ba-$Fe^{III}W_{12}$** at 259 and 257 nm, respectively. Note that no maximum is seen for **NH_4-$Fe^{III}W_{11}Ni^{II}$**. The UV spectra of aqueous solutions ($c \approx 1.6 \times 10^{-5}$ mol/L) of **NH_4-$ZnW_{11}Zn$**, **Na-PT**, and **NH_4-MT** are shown below, (b). A characteristic maximum (λ_{max}) was observed only for **NH_4-MT** at 257 nm. No maxima were found for **NH_4-$ZnW_{11}Zn$** and **Na-PT**.

ion.[37] The UV spectrum of **NH_4-$Fe^{III}W_{11}Ni^{II}$** in comparison to that of **K-$SiW_{11}Fe^{III}$** (Fe^{III} in peripheral distorted octahedral coordination) and **Ba-$Fe^{III}W_{12}$** (Fe^{III} in central tetrahedral coordination) is shown in Figure 7a. Both **K-$SiW_{11}Fe^{III}$** and **Ba-$Fe^{III}W_{12}$** (Keggin-type POTs) exhibit the characteristic maximum of the W ← O charge-transfer band at 259 and 257 nm with $\epsilon = 3.3 \times 10^4$ and 3.7×10^4 L(mol·cm)$^{-1}$, respectively. In contrast, no maximum is observed for **NH_4-$Fe^{III}W_{11}Ni^{II}$**. A comparison of the UV spectra of **NH_4-$Zn^{II}W_{11}Zn^{II}$** with **NH_4-PT** (paratungstate B), and **NH_4-MT** (metatungstate), Figure 7b, reveals a similar result. Again, a maximum is observed for **NH_4-MT** (Keggin-type) at 256 nm ($\epsilon = 3.8 \times 10^4$ L(mol·cm)$^{-1}$), but not for **NH_4-PT** (paratungstate B), which is known to exist in solution only in equilibrium with the heptatungstate (paratungstate A).[15,16,31] The UV spectrum of **NH_4-$Zn^{II}W_{11}Zn^{II}$** also shows no maximum and is almost identical to that observed for **NH_4-PT**, Figure 7b.

These observations raised the question whether the investigated M(3d)W_{11}M′(3d) POTs actually exist in solution as *intact* Keggin ions or if the anions (i.e., as in sodium paratungstate B) may be formed only during the crystallization process. Further investigations were carried out comparing the UV spectra of **NH_4-$Zn^{II}W_{11}Ni^{II}$** with **K-SiW_{11}** (lacunary Keggin structure, α-isomer), and the corresponding **K-$SiW_{11}Ni^{II}$** complex (with Ni^{II} in peripheral octahedral coordination).

Absorption spectra for the visible region (400−800 nm) for the M(3d)W_{11}M′(3d) complexes are summarized in Figure 8a and b. Three typical absorptions at 413, 468, and

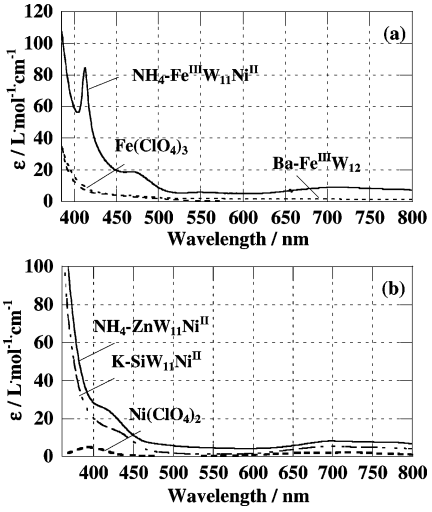

Figure 8. Vis spectra of **NH_4-$Fe^{III}W_{11}Ni^{II}$** ($c \approx 0.01$ mol/L), **Ba-$Fe^{III}W_{12}$** ($c \approx 0.05$ mol/L), and $Fe(ClO_4)_3$ ($c \approx 0.09$ mol/L) in aqueous solution, (a). Note that no absorption indicating tetrahedrally coordinated Ni^{2+} could be observed. A comparison of **NH_4-$ZnW_{11}Ni^{II}$** ($c \approx 0.02$ mol/L), **K-$SiW_{11}Ni^{II}$** ($c \approx 0.02$ mol/L), and $Ni(ClO_4)_2$ ($c \approx 0.05$ mol/l), all Ni^{2+} in octahedral coordination, is shown in (b).

711 nm are observed for **NH_4-$Fe^{III}W_{11}Ni^{II}$** with molar extinction coefficients, ϵ, of approximately 85, 19, and 9 L(mol·cm)$^{-1}$, respectively. Three spin-allowed transitions are expected for octahedral Ni^{2+} (d_8), thus the absorption bands at ∼413 (24 213 cm^{-1}) and 711 nm (14 064 cm^{-1}) may be assigned to $^3A_{2g} \rightarrow {}^3T_{1g}(P)$ and $^3A_{2g} \rightarrow {}^3T_{1g}(F)$ transitions, respectively. A regular $\{Ni^{II}O_4\}$ tetrahedron located in the center of an intact Keggin structure should result in a $^3T_1(F)$ ground state, and the transition to the $^3T(P)$ state should occur in the visible region at ∼15 000 cm^{-1}.[38] The expected transition is relatively strong ($\epsilon \approx 10^2$ L(mol·cm)$^{-1}$) compared to the corresponding $^3A_{2g} \rightarrow {}^3T_{1g}$ in octahedral coordination. Hence, the noticeable absence of such a characteristic feature in the visible spectra of **NH_4-$Fe^{III}W_{11}Ni^{II}$** provides further evidence that the "[α-$Fe^{III}O_4W_{11}O_{30}Ni^{II}O_5(OH_2)]^{7-}$" Keggin anion does not exist as an intact structural unit in solution.[39] The tendency of Fe(III) to have charge-transfer bands in the near-UV region obscures the very weak, spin-forbidden $d-d$ bands. As expected, no distinct features are observed for **Ba-$Fe^{III}W_{12}$**, and $Fe(ClO_4)_3$, Figure 8a. A comparison between **NH_4-$ZnW_{11}Ni^{II}$**, **K-$SiW_{11}Ni^{II}$**, and $Ni(ClO_4)_2$ is shown in Figure 8b. The visible spectrum of **NH_4-$ZnW_{11}Ni^{II}$** appears indeed very similar to that of **K-$SiW_{11}Ni^{II}$**, indicating that all of the Ni^{II} is situated in an octahedral coordination, as expected for Ni^{II} in a peripheral position of an intact Keggin anion (i.e., in **K-$SiW_{11}Ni^{II}$**) or of $Ni(OH_2)_6^{2+}$. The molar extinction coefficients observed in the UV spectroscopic studies, vide supra, differ from those in the vis spectroscopic studies by several orders of magnitude; hence, a control experiment was carried out in order

(37) (a) Nomiya, K.; Kobayashi, R.; Miwa, M. *Bull. Chem. Soc. Jpn.* **1983**, *56*, 2272−2275. (b) Nomiya, K.; Miwa, M.; Kobayashi, R.; Aiso, M. *Bull. Chem. Soc. Jpn.* **1981**, *54*, 2983−2987. (c) Tourné, C. M.; Tourné, G. F.; Malik, S. A.; Weakley, T. J. R. *Inorg. Nucl. Chem.* **1970**, *32*, 3875−3890.

(38) Cotton, F. A., Wilkinson, G., Murillo, C. A., Bochmann, M., Eds.; *Advanced Inorganic Chemistry*, 6th ed.; John Wiley and Sons: New York, 1999; pp 838−842.

(39) (a) Ripan, R.; Puşcaşiu, M. *Z. Anorg. Allg. Chem.* **1971**, *380*, 102−106. (b) Ripan, R.; Duca, A.; Stănescu, D.; Puşcaşiu, M. *Z. Anorg. Allg. Chem.* **1966**, *347*, 333−336. (c) Ripan, R.; Puşcaşiu, M. *Z. Anorg. Allg. Chem.* **1968**, *358*, 82−89.

Scheme 1. Synthesis Routes for $(NH_4)_6Ni^{II}_{0.5}[\alpha\text{-}Fe^{III}O_4W_{11}O_{35}Ni^{II}(OH_2)]\cdot\sim 18H_2O$[a]

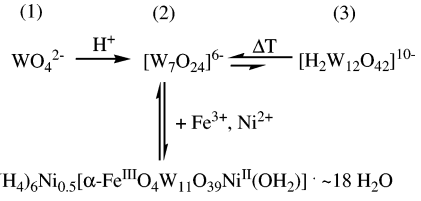

[a] (1) *General Synthesis*, Na_2WO_4/H^+; (2) *Alternative Synthesis A*, $Na_6[W_7O_{24}]$ (paratungstate A); (3) *Alternative Synthesis B*, $Na_{10}[H_2W_{12}O_{42}]$ (paratungstate B).

to investigate whether spectral changes could be observed as function of the different concentrations. An aqueous solution of constant concentration (5×10^{-3} M) of all four M(3d)W_{11}M′(3d) complexes was measured using path lengths from 0.01 to 1.0 cm. No concentration-dependent differences were seen when compared to the original UV (diluted) and UV−vis (more-concentrated) spectra. A summary of the UV spectroscopic data is provided in Tables S8 and S9, and Figures S8-1 and S10 of the Supporting Information.

Control Experiments for the Presence of "Free", Cationic M^{n+} (M = 3d) in the Aqueous Solutions of NH_4-M(3d)W_{11}M′(3d). The addition of aqueous dimethylglyoxime (sodium salt) to the solutions of **NH_4-$Fe^{III}W_{11}Ni^{II}$**, **NH_4-$ZnW_{11}Ni^{II}$**, and **NH_4-$Co^{II}W_{11}Ni^{II}$** at pH 6.8 caused the immediate formation of a red-pink precipitate in all three experiments, indicating the formation of the characteristic nickel dimethylglyoxime complex due to the presence of "free" or weakly bound Ni^{2+} ions. In contrast, no reaction is seen upon addition of dimethylglyoxime to a solution of **K-$SiW_{11}Ni^{II}$**, thus confirming the stability of the *intact* $[SiO_4W_{11}O_{35}Ni^{II}(OH_2)]^{6-}$ anion. The addition of dimethylglyoxime was repeated after adjustment of the pH to ∼3.0. Again, the formation of insoluble nickel dimethylglyoxime was observed for the M(3d)W_{11}M′(3d) complexes, which can now be explained with the formation of the MW_{12} complexes (M = Fe^{3+}, Zn^{2+}, and Co^{2+}) at the lower pH.

Addition of aqueous potassium thiocyanate, KSCN, to solutions of **NH_4-$Fe^{III}W_{11}Ni^{II}$** and **NH_4-$ZnW_{11}Fe^{III}$** (pH ≈ 6.8) did not result in the formation of the dark-red iron(III) thiocyanate complex, indicating that no "free" or weakly bound Fe^{3+} remained in solution. This is consistent with the presence of the lacunary $[Fe^{III}O_4W_{11}O_{35}]^{9-}$ anion in the aqueous solutions of both M(3d)W_{11}M′(3d) complexes. However, the addition of KSCN to an *acidified* (pH ≈ 3.0) solution of **NH_4-$ZnW_{11}Fe^{III}$** did produce the deep-red iron(III) thiocyanate complex, thus indicating the formation of the more-stable ZnW_{12} complex (and "free" Fe^{3+}), rather than $Fe^{III}W_{12}$ (and "free" Zn^{2+}). No reaction was observed for the acidified solutions of **NH_4-$Fe^{III}W_{11}Ni^{II}$**, which is consistent with the formation of **NH_4-$Fe^{III}W_{12}$** (and "free" Ni^{2+}) from **NH_4-$Fe^{III}W_{11}Ni^{II}$**; hence, the formation of *solid* **NH_4-$Fe^{III}W_{11}Ni^{II}$**, vide supra, can easily be rationalized by reaction of a lacunary $[Fe^{III}O_4W_{11}O_{35}]^{9-}$ heteropolytungstate with Ni^{2+} (i.e., Scheme 1). No reaction with KSCN is seen upon addition to solutions of **K-$SiW_{11}Fe^{III}$** (with and without acidification), thus confirming the stability of the *intact* $[SiO_4W_{11}O_{35}Fe^{III}(OH_2)]^{5-}$ heteropolytungstate anion. In summary, the above control experiments by themselves provide good evidence that M(3d)W_{11}M′(3d) complexes are either of low stability or do not exist as intact structural units in their aqueous solutions. The addition of acid leads to the formation of the corresponding, more-stable MW_{12} complexes (M = Fe^{3+}, Zn^{2+}, Co^{2+}) and "free" Ni^{2+} or Fe^{3+}. Additional experimental details are provided in Table S11 and Figure S12 of the Supporting Information.

Summary. The POT complexes $(NH_4)_6Ni^{II}_{0.5}$-$[\alpha\text{-}Fe^{III}O_4W_{11}O_{30}Ni^{II}O_5(OH_2)]\cdot 18H_2O$, $(NH_4)_7Zn_{0.5}[\alpha\text{-}ZnO_4\text{-}W_{11}O_{30}ZnO_5(OH_2)]\cdot 18H_2O$, and $(NH_4)_7Ni^{II}_{0.5}[\alpha\text{-}ZnO_4W_{11}O_{30}\text{-}Ni^{II}O_5(OH_2)]\cdot 18H_2O$ could equally be obtained using aqueous solutions of either Na_2WO_4 at pH ≈ 7, $Na_6[W_7O_{24}]\cdot\sim 14H_2O$, or $Na_{10}[H_2W_{12}O_{42}]\cdot 27H_2O$ as starting materials. The summary of the three synthesis routes leading to $(NH_4)_6Ni^{II}_{0.5}$-$[\alpha\text{-}Fe^{III}O_4W_{11}O_{30}Ni^{II}O_5(OH_2)]\cdot 18H_2O$ (as an example) is provided in Scheme 1.

The 3d-metal ions are distributed over three different positions, namely the central (tetrahedral) position, the peripheral (octahedral) positions of the Keggin anion, and cationic positions outside of the POT framework. The results of UV−vis spectroscopy, solution (^{1}H, ^{183}W) NMR, and solid-state (^{1}H) NMR suggest that the investigated transition-metal-disubstituted POTs exist in neutral solution in complex equilibria of transition metal cations, $[W_7O_{24}]^{6-}$ (heptatungstate), and lacunary Keggin anions, $[H_xM^{m+}W_{11}O_{39}]^{n-}$ (undecatungstates). For example, aqueous solutions of **NH_4-$Fe^{III}W_{11}Ni^{II}$** are largely composed of hydrated Ni^{2+} cations and the lacunary Keggin anion $[Fe^{III}O_4W_{11}O_{39}]^{9-}$. **$NH_4$-$ZnW_{11}Ni^{II}$** and **$NH_4$-$ZnW_{11}Zn$** appear to exist in solution as mixtures of the hydrated transition metal cations (Zn^{2+}, Ni^{2+}) and $[W_7O_{24}]^{6-}$. At pH < 4 the corresponding, thermodynamically more stable MW_{12} Keggin anions (M = Fe^{3+}, Zn^{2+}, Co^{2+}) are formed which can readily be isolated. The formation, as well as distribution, of the POT species in solution may be influenced by ion-pairing effects due to the presence of the transition metal counterions. The 3d-metal-disubstituted Keggin anions are not being formed until the crystallization process.

Acknowledgment. We would like to thank Prof. R. Stösser, Department of Chemistry, Humboldt University, Berlin, Germany for helpful discussions on the ESR spectra; we also thank Dr. J. Petersen, Department of Chemistry, West Virginia State University, for his help in the verification of previously obtained ESR data. We are thankful to Dr. S. Erskine, The Dow Chemical Company, for collecting the Raman spectra. We also acknowledge Dr. S. Roychowdhury, OSRAM Sylvania, for carrying out the chemical analyses and Dr. A. Harrison and Dr. J. Xiong, The Dow Chemical Company, for carrying out ^{183}W NMR and ^{1}H-MAS NMR experiments.

Supporting Information Available: Tables S1 and S2, summary and additional references of relevant literature on 1:11:1 POMs containing two metals as heteroelements (11 pages); additional

(40) (a) Tytko, K. H.; Baethe, G.; Cruywagen, J. J. *Inorg. Chem.* **1985**, *24*, 3132−3136. (b) Yagasaki, A.; Anderson, I.; Pettersson, L. *Inorg. Chem.* **1987**, *26*, 392−396.

experiments concerning the synthesis of **NH_4-$ZnW_{11}Fe^{III}$**, **NH_4-$Co^{II}W_{11}Ni^{II}$**, and trials for **NH_4-$Fe^{III}W_{11}Fe^{III}$** and **NH_4-$Ni^{II}W_{11}Ni^{II}$** POMs (2 pages); Table S3, elemental analysis data and calculated compositions (1 page); Figure S4, ^{1}H-MAS NMR spectra of **K-MT**, **K-PT**, and **K-$ZnW_{11}Zn$** (1 page); Figure S5 and Table S5-1, ^{1}H NMR spectra and experimental conditions for the detection of metatungstate (2 pages); Table S6 and Figure S6-1, experimental details, corresponding ^{183}W NMR, and ^{31}P NMR spectra of **NH_4-$ZnW_{11}Zn$**, **NH_4-PT**, and **NH_4-PW_{11}** (2 pages); Figure S7, IR spectra for **TBA-MW_{12}** (M = Fe^{III}, Co^{II}, Zn^{II}) POTs (1 page); Table S8 and Figure S8-1, summary of UV spectroscopic data (2 pages); Table S9, summary of vis spectroscopic data (1 page); Figure S10, UV−vis spectra of M(3d)W_{11}M′(3d) complexes at constant concentration (1 page); Table S11, control experiments and their implication on the structural composition of the M(3d)-W_{11}M′(3d) complexes (1 page); Figure S12, UV spectra showing the conversion of the M(3d)W_{11}M′(3d) polyoxotungstates to the corresponding MW_{12} Keggin structures upon acidification (1 page). This material is available free of charge via the Internet at http://pubs.acs.org.

IC048155L